Electronic Supplementary Material (ESI) for ChemComm.

Supporting Information

for

New mechanistic insight into intramolecular aromatic ligand hydroxylation and benzyl alcohol oxidation initiated by well-defined (μ-peroxo)diiron(III) complex

Mio Sekino, Hideki Furutachi, Rina Tojo, Ayumi Hishi, Hanako Kajikawa, Takatoshi Suzuki, Kaito Suzuki, Shuhei Fujinami, Shigehisa Akine, Yoko Sakata, Takehiro Ohta, Shinya Hayami, and Masatatsu Suzuki

Contents:

Figure S1. Benzyl alcohol concentration dependence on the molar absorption coefficient values (ε, 577 nm) of decomposed solution of **1**-O_2 in dichloromethane at 25˚C.

Figure S2. An ORTEP view (50 % probability) of $[Fe_2(L^{Ph4})(O_2)(Ph_3CCO_2)(CH_3OH)]^{2+}$ (**1**-O_2-MeOH) with a full numbering scheme of atoms. Most hydrogen atoms and all solvent molecules are omitted for clarity.

Figure S3. Space-filling representations of $[Fe_2(L^{Ph4})(O_2)(Ph_3CCO_2)(CH_3OH)]^{2+}$ (**1**-O_2-MeOH) (A: X-ray) and its CH_2Cl_2 adduct (B: X-ray).

Figure S4. Overlays of X-ray crystal (ball-and-stick) and DFT-optimized (B3LYP: aqua tube, BP86: gray tube, BP86 with 10% Hartree-Fock mixing: orange tube) structures of $[Fe_2(L^{Ph4})(O_2)(Ph_3CCO_2)(CH_3OH)]^{2+}$ (**1**-O_2-MeOH).

Table S1. The 1st-coordination sphere structures of **1**-O_2-MeOH (X-ray) and DFT-optimized **1**-O_2-MeOH.

Figure S5. Mössbauer spectrum of a powdered sample of **1**-O_2-MeOH at 80K.

Figure S6. Electronic spectral change for decomposition of **1**-O_2 (0.56 mM) in the absence of benzyl alcohol (A) and in the presence of benzyl alcohol (0.56 M, 1000 equiv.) (B) in dichloromethane at 25 °C . Insets: Decay time profile of the absorbance at 668 nm (curve) and pseudo-first order plot (liner plot).

Table S2. Kinetic parameters for the reaction of **1**-O_2 with benzyl alcohol at 25 ºC.

Figure S7. Plot of k_{obs} against concentrations of 9,10-DHA (0.17 M), toluene (0.52 M), styrene (0.52 M), and benzyl alcohol (0.56 M) in CH_2Cl_2 at 25˚C.

Table S3. Kinetic parameters for the reaction of **1**-O_2 with various substrates at 25 ºC.

Figure S8. ESI-TOF mass spectra of HL^{Ph4}-^{16}OH (A), HL^{Ph4}-^{18}OH (B), and HL^{Ph4}-$^{16/18}OH$ (C) obtained from decomposed dichloromethane solutions of **1**-O_2 prepared by $^{16}O_2$, $^{18}O_2$, and $^{16}O_2$ in the presence of 1000 equiv. of $H_2{}^{18}O$ (diluted with MeCN) at 25 °C. (D) Calculated isotope pattern of (C).

Materials. Dinucleating ligand (HL^{Ph4} = *N*,*N*,*N'*,*N'*-tetrakis(1-methyl-2-phenyl-4-imidazolyl)methyl-1,3-amino-2-propanol) and diiron(II) complex $[Fe_2(L^{Ph4})(Ph_3CCO_2)]^{2+}$ (**1**) were synthesized according to the literature methods (M. Yamashita, *J. Am. Chem Soc.* 2007, **129**, 2-3). CH_2Cl_2 was dried over CaH_2 and distilled under N_2 before use. $^{18}O_2$ (95% ^{18}O-enriched) and $H_2{}^{18}O$ (≧98% ^{18}O-enriched) were purchased from TAIYO NIPPON SANSO Corporation (Tokyo, Japan). 9,10-DHA was recrystallized three times from EtOH under N_2. Toluene was washed with cold concentrated H_2SO_4 (once), water (three times), 10% $NaHCO_3$ (three times), and water again (three times), after which they were dried over $MgSO_4$ and then distilled under N_2 in the presence of Na. Styrene was washed with 5 % NaOH aqueous solution, washed with water (3 times), and dried with $MgSO_4$ and passed through a short alumina column before use. Benzyl alcohol and benzyl alcohol-d_7 were distilled under reduced pressure in the presence of $NaBH_4$. All other reagents and solvents were commercially available and used without further purification.

Isolation of $[Fe_2(L^{Ph4})(O_2)(Ph_3CCO_2)(MeOH)](BPh_4)_2$ (1-O_2-MeOH). To a mixture of dichloromethane (4 ml) and acetonitrile (2 ml) containing $[Fe_2(L^{Ph4})(Ph_3CCO_2)](ClO_4)_2 \cdot 3H_2O$ (**1**) (150 mg, 0.11 mmol) was injected O_2 at −80 °C to give a dark green solution. The resulting dark green solution was stirred for 20 minutes under O_2 and addition of a methanol solution (6 ml) of $NaBPh_4$ (188 mg, 0.55 mmol) afforded a dark green powder. Single crystals of **1**-O_2-MeOH suitable for X-ray crystallography were obtained from the above mixture at −80 °C. Mössbauer spectrum of a polycrystalline sample of **1**-O_2-MeOH at 80K: $\delta(\Delta E_Q)$ = 0.57 (1.47) and 0.59 (0.90) mm/s (Fig. S5).

Kinetic measurements. The rates of decay of **1**-O_2 (~0.56 mM) in the presence of various concentrations of the external substrates 9,10-DHA (~0.17 M), toluene (~0.56 M), styrene (~0.56 M), and benzyl alcohol (0 ~ 0.56 M) in dichloromethane at 25 ˚C under O_2 were measured by monitoring the spectral change at 668 nm using a Shimadzu diode array Multispec-1500 spectrometer. A dichloromethane solution of **1** was kept at desired temperature for 20 minutes and oxygenated by bubbling of O_2 for 30 seconds to give a dark green **1**-O_2. Subsequently, to the resulting solution was added a dichloromethane solution containing external substrates mentioned above. Decompositions of **1**-O_2 under the conditions obeyed pseudo-first-order kinetics and the rates constants (k_{obs}) were determined by least-squares curve fitting (Fig. S6). The decomposition rates of **1**-O_2 were independent on various concentrations of the external substrates (Figs. 3 and S7, Tables S2 and S3).

Product analysis by GC-MS. Products formed in the reactions of **1**-O_2 with 9,10-DHA, toluene, styrene, and benzyl alcohol, were analyzed by comparison of the mass peaks and retention time of the products with respect to authentic samples. Only the reaction of **1**-O_2 with

benzyl alcohol afforded an oxidation product, benzaldehyde, however, any oxidation products were not detected in the reactions of **1**-O_2 with the other substrates. After the reaction of **1**-O_2 with benzyl alcohol (300 equiv. or 600 equiv.) or benzyl alcohol (300 equiv.)/d_7-benzyl alcohol (300 equiv.) mixture, the reaction mixture was passed through a short silica-gel column and eluted with dichloromethane. A known concentration of bromobenzene was added to the eluent as an internal standard. The yields of benzaldehyde were determined by comparison against standard curves prepared with a known authentic sample. Yields of benzaldehyde in the reaction of **1**-O_2 with 300 equiv. and 600 equiv. of benzyl alcohol were ~170% and ~280%, respectively.

^{18}O Labeling experiments. Hydroxylation of ligand HL^{Ph4} was carried out using $^{16}O_2$ in the presence of $H_2{}^{18}O$ (1000 equiv.) or $H_2{}^{18}O$ (1000 equiv.)/benzyl alcohol (1000 equiv.) mixture. A dichloromethane solution of **1** was oxygenated by bubbling of O_2 to give a dark green **1**-O_2 at 25 °C. Subsequently, to the resulting solution was added an acetonitrile solution containing $H_2{}^{18}O$ (1000 equiv.) or $H_2{}^{18}O$ (1000 equiv.)/benzyl alcohol (1000 equiv.) mixture. After the reaction was completed, the mixtures were worked up according to the published ligand recovery method (M. Yamashita, *J. Am. Chem Soc.* 2007, **129**, 2-3). Formation of HL^{Ph4}-$^{16/18}$OH was identified by ESI-MS (Figure S8 (C)). ESI-TOF mass spectrum of HL^{Ph4}-OH obtained from decomposed dichloromethane solutions of **1**-O_2 prepared by $^{16}O_2$ in the presence of 1000 equiv. of $H_2{}^{18}O$/1000 equiv. of benzyl alcohol was same to that of Figure S8 (A).

Physical measurements. Electronic spectra were measured with a Shimadzu diode array Multispec-1500 spectrometer. The temperatures were controlled with a water-circulating cell holder attached with a circulating pump (ADVANTEC LCH-4V). ESI-TOF/MS spectra were measured with a Micromass LCT spectrometer. GC-MS analysis was performed on a Shimadzu GCMS-QP2010 plus. GC-MS instrument equipped with a fused slilica capillary column (100% dimethylpolysiloxane, 0.32 mm diameter × 25 m, QUADREX Corp.). ^{1}H NMR spectra were measured with JEOL LNM-LM400 using tetramethylsilane (TMS) as the internal standard. Mössbauer spectrum was measured with S-600 constant-acceleration spectrum (Austin Science Associates) at 80 K. Temperature was controlled with a temperature controller (ITC502, Oxford Instruments) within a variable temperature cryostat (DN1726, Oxford Instruments). The powdered sample was loaded in a sample holder cooled on dry ice. The data were stored in a 1024-channel analyzer (IT-5200, Inotech Inc.). A 10 mCi cobalt-57 source diffused into a palladium foil was used. The velocity scales and isomer shifts were normalized to iron foil at room temperature.

X-ray crystallography. A single crystal was picked up from the solution by a nylon loop on a hand-made copper plate mounted inside a liquid N_2 Dewar vessel ca. –80 ˚C. Then the crystal was mounted on a goniometer head in a N_2 cryosteam. X-ray diffraction study for

$[Fe_2(L^{Ph4})(O_2)(Ph_3CCO_2)(CH_3OH)](BPh_4)_2 \cdot 3.4CH_3CN \cdot 9.5CH_2Cl_2 \cdot 3.3CH_3OH$ (**1**-O_2-MeOH) was made on a Rigaku/MSC Mercury diffractometer with graphite monochromated Mo-Kα radiation (λ = 0.71073 Å). The data were collected at –150 ˚C and corrected for Lorentz and polarization effects. Empirical absorption corrections were applied. The structure of **1**-O_2-MeOH was solved by a direct method (SIR92)[1] The structure was refined by a full-matrix least-squares method by using the SHELXL 2014[2] (Yadokari-XG[3]). **1**-O_2-MeOH always produced poorly diffracting very thin crystals and one effort resulted in data collection and structure solution. The molecular structure of **1**-O_2-MeOH with a numbering scheme of atoms is shown in Figure S2. The crystallographic data and tables of final atomic coordinates, thermal parameters, and full bond distances and angles are given in CIF (CCDC 1554479).

[1] *SIR92*: A. Altomare, G. Cascarano, C. Giacovazzo, A. Guagliardi, M. C. Burla, G.Polidori, M. Camalli, *J. Appl. Crystallogr*., 1994, **27**, 435.
[2] G. M. Sheldrick, SHELXL-2014; G. M. Sheldrick, *Acta. Crystallogr.*, 2008, **A64**, 112.
[3] Yadokari-XG, Software for Crystal Structure Analyses, K. Wakita (2001); Release of Software Yadokari-XG (2009) for Crystal Structure Analyses, C. Kabuto, S. Akine, T. Nemoto, and E. Kwon, *J. Cryst. Soc. Jpn.*, 2009, **51**, 218.

DFT calculation. All computations were carried out using Gaussian09 program computational package.[1] The initial coordinate for geometry optimizations was taken from the crystal structure. The diferric center (S = 0) was computed with the broken-symmetry formalism[2,3] with B3LYP, BP86, and BP86 functional with 10% Hartree-Fock exchange, in combination with the 6-31g* basis set. The BP86 functional combined with 10% Hartree-Fock exchange was shown to be in reasonable agreement with spectroscopic data for diiron models.[4] The geometry optimizations and calculations of Hessians at the same theory level were performed. The Hessian analyses confirmed that the DFT optimized structures are the ground state structures. The overall structures are consistent with the crystal structure (Figure S4), while the details are sensitive to the functionals. All DFT calculations over- and underestimate the Fe–O and O–O bond covalency, respectively, compared to the crystal structure (Table S1). Significant deviations can be seen in the positions of phenyl rings from the overlay plots (Figure S4), possibly due to the lack of the dispersion and crystal packing forces in the computations. The calculated position of the carbon atom of methanol is also slightly off from the crystal structure, while the H-bond interaction between the OH group of methanol with the nitrogen atom of imidazole moiety is reproduced in the calculations. X-ray structural analysis of **1**-O_2-MeOH revealed that a CH_2Cl_2 molecule locates in a hydrophobic cavity formed by phenyl groups (Figure S3 (B)). Nevertheless, the DFT-calculated structural features agree with its X-ray

structural feature (Figure S4), except for the deviations of positions of phenyl rings mentioned above.

[1] Gaussian 09, Revision E.01, M. J. Frisch, G. W. Trucks, H. B. Schlegel, G. E. Scuseria, M. A. Robb, J. R. Cheeseman, G. Scalmani, V. Barone, B. Mennucci, G. A. Petersson, H. Nakatsuji, M. Caricato, X. Li, H. P. Hratchian, A. F. Izmaylov, J. Bloino, G. Zheng, J. L. Sonnenberg, M. Hada, M. Ehara, K. Toyota, R. Fukuda, J. Hasegawa, M. Ishida, T. Nakajima, Y. Honda, O. Kitao, H. Nakai, T. Vreven, J. A. Montgomery, Jr., J. E. Peralta, F. Ogliaro, M. Bearpark, J. J. Heyd, E. Brothers, K. N. Kudin, V. N. Staroverov, T. Keith, R. Kobayashi, J. Normand, K. Raghavachari, A. Rendell, J. C. Burant, S. S. Iyengar, J. Tomasi, M. Cossi, N. Rega, J. M. Millam, M. Klene, J. E. Knox, J. B. Cross, V. Bakken, C. Adamo, J. Jaramillo, R. Gomperts, R. E. Stratmann, O. Yazyev, A. J. Austin, R. Cammi, C. Pomelli, J. W. Ochterski, R. L. Martin, K. Morokuma, V. G. Zakrzewski, G. A. Voth, P. Salvador, J. J. Dannenberg, S. Dapprich, A. D. Daniels, O. Farkas, J. B. Foresman, J. V. Ortiz, J. Cioslowski, and D. J. Fox, Gaussian, Inc., Wallingford CT, 2013.
[2] K. Yamaguchi, F. Jensen, A. Dorigo, K. Houk, *Chem. Phys. Lett.*, 1988, **149**, 537–542.
[3] W.-G. Han and L. Noodleman, *Inorg. Chem.*, 2011, **50**, 2302-2320.
[4] K. Park, T. Tsugawa, H. Furutachi, Y. Kwak, L. V. Liu, S. D.Wong, Y. Yoda, Y. Kobayashi, M. Saito, M. Kurokuzu, M. Seto, M. Suzuki, and E. I. Solomon, *Angew. Chem. Int. Ed.*, 2013, **52**, 1294-1298.

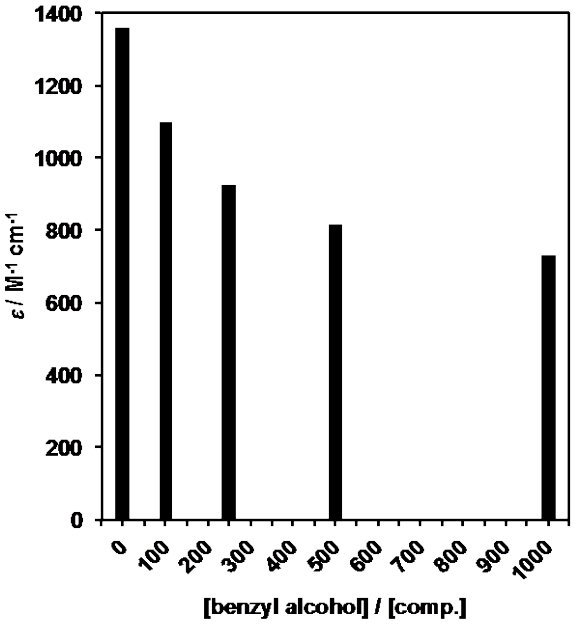

Figure S1. Benzyl alcohol concentration dependence on the molar absorption coefficient values (ε, 577 nm) of decomposed solution of **1**-O_2 in dichloromethane at 25˚C.

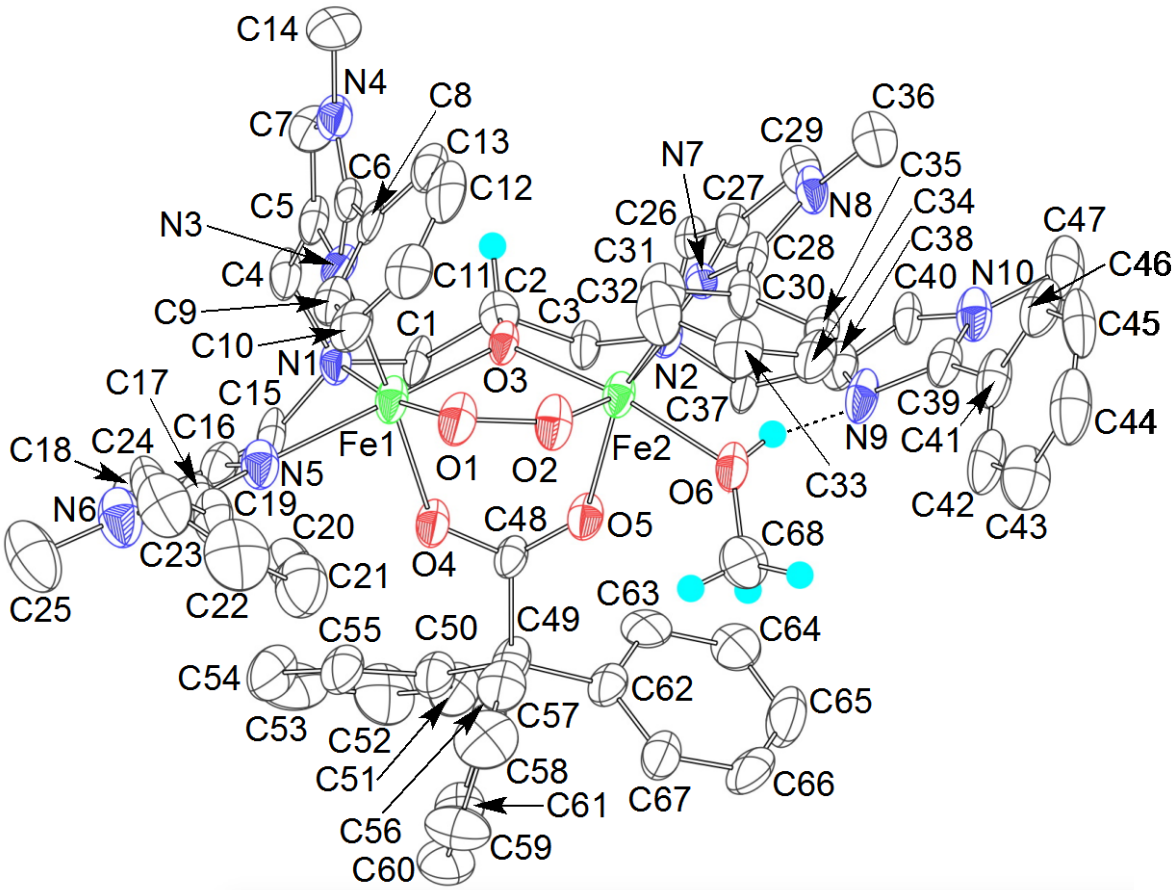

Figure S2. An ORTEP view (50 % probability) of $[Fe_2(L^{Ph4})(O_2)(Ph_3CCO_2)(CH_3OH)]^{2+}$ (**1**-O_2-MeOH) with a full numbering scheme of atoms. Most hydrogen atoms and all solvent molecules are omitted for clarity.

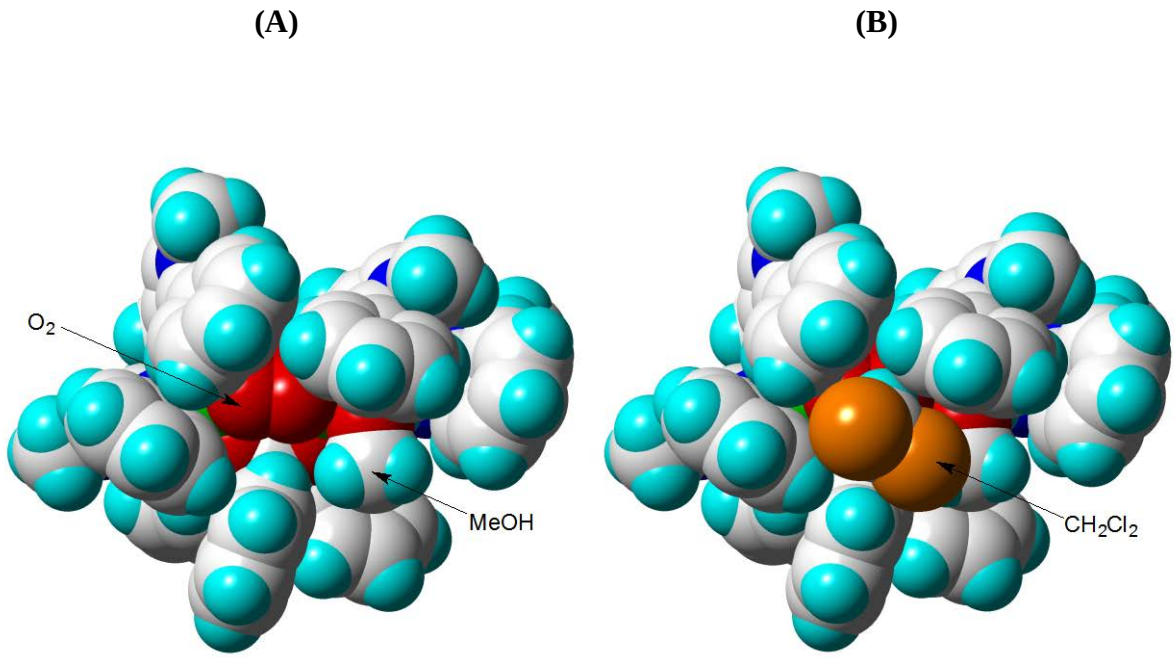

Figure S3. Space-filling representations of $[Fe_2(L^{Ph4})(O_2)(Ph_3CCO_2)(CH_3OH)]^{2+}$ (**1**-O_2-MeOH) (A: X-ray) and its CH_2Cl_2 adduct (B: X-ray).

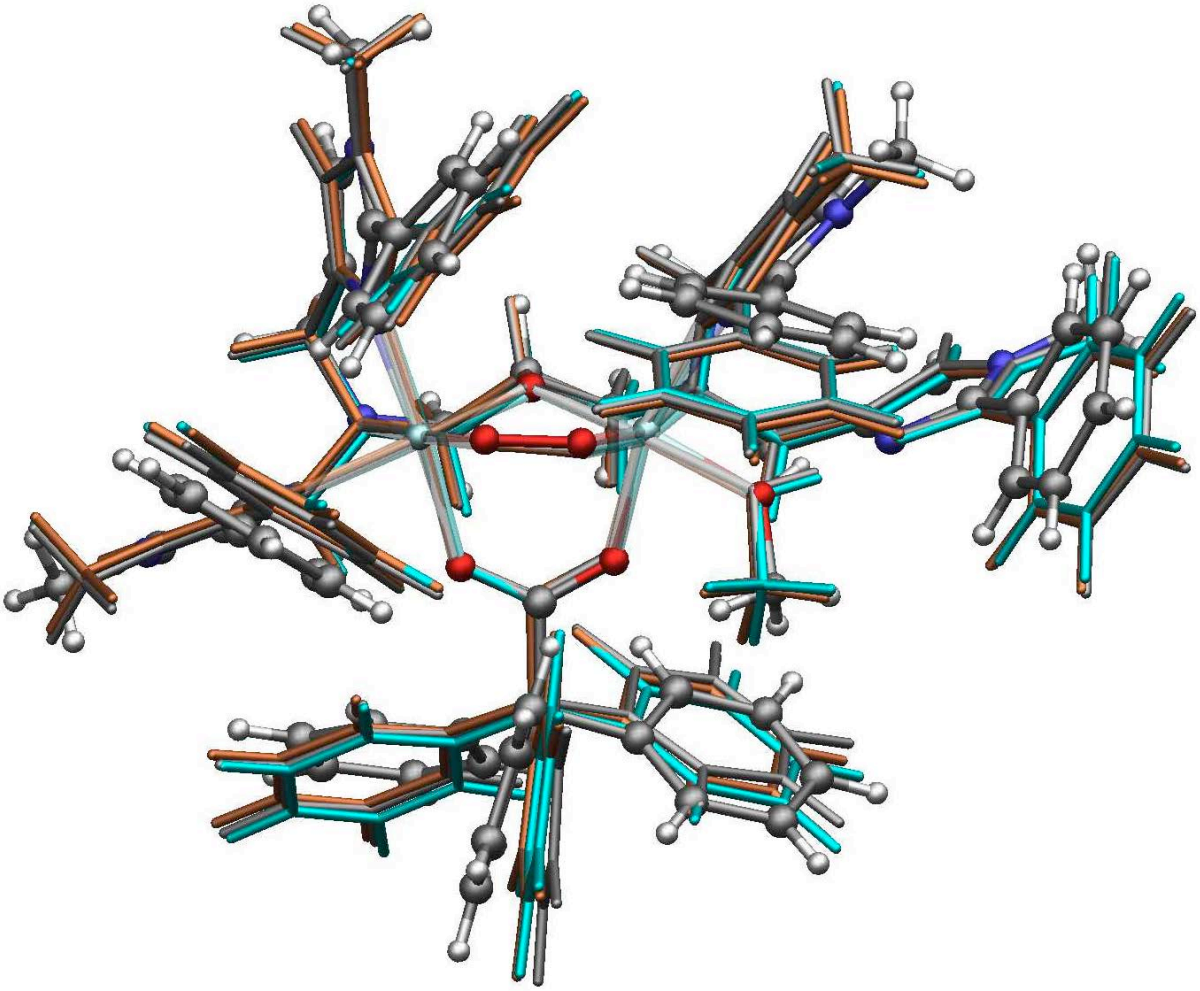

Figure S4. Overlays of X-ray crystal (ball-and-stick) and DFT-optimized (B3LYP: aqua tube, BP86: gray tube, BP86 with 10% Hartree-Fock mixing: orange tube) structures of $[Fe_2(L^{Ph4})(O_2)(Ph_3CCO_2)(CH_3OH)]^{2+}$ (**1**-O_2-MeOH).

Table S1. The 1st-coordination sphere structures of **1**-O_2-MeOH (X-ray) and DFT-optimized **1**-O_2-MeOH.

	Distances (Å)			
	X-ray	DFT		
		B3LYP	BP86	BP86*
O1–O2	1.40	1.42	1.47	1.42
Fe1–O1	1.85	1.76	1.75	1.76
Fe1–O3	2.01	1.91	1.92	1.91
Fe1–O4	2.08	1.96	1.94	1.95
Fe1–N1	2.24	2.10	2.08	2.08
Fe1–N3	2.14	2.04	2.01	2.01
Fe1–N5	2.13	2.04	2.00	2.01
Fe2–O2	1.88	1.79	1.76	1.78
Fe2–O3	1.99	1.92	1.92	1.91
Fe2–O5	2.06	1.93	1.90	1.91
Fe2–O6	2.03	1.98	1.99	1.97
Fe2–N2	2.30	2.20	2.18	2.17
Fe2–N7	2.12	2.01	1.98	1.98
Fe1•••Fe2	3.31	3.15	3.17	3.14
	Angles (deg)			
Fe1–O3–Fe2	111.7	110.2	111.2	110.7
Fe1–O1–O2	118.7	117.6	117.6	117.7
Fe2–O2–O1	122.6	120.0	120.3	120.4
Fe1–O1–O2–Fe2	7.0	12.1	7.6	8.6

* 10% Hartree-Fock mixing

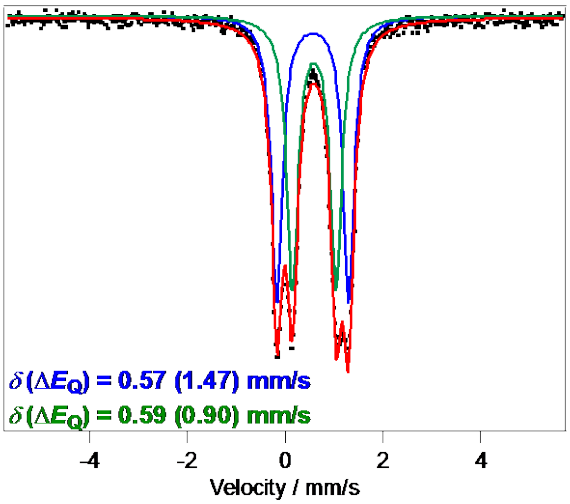

Figure S5. Mössbauer spectrum of a powdered sample of **1**-O_2-MeOH at 80K.

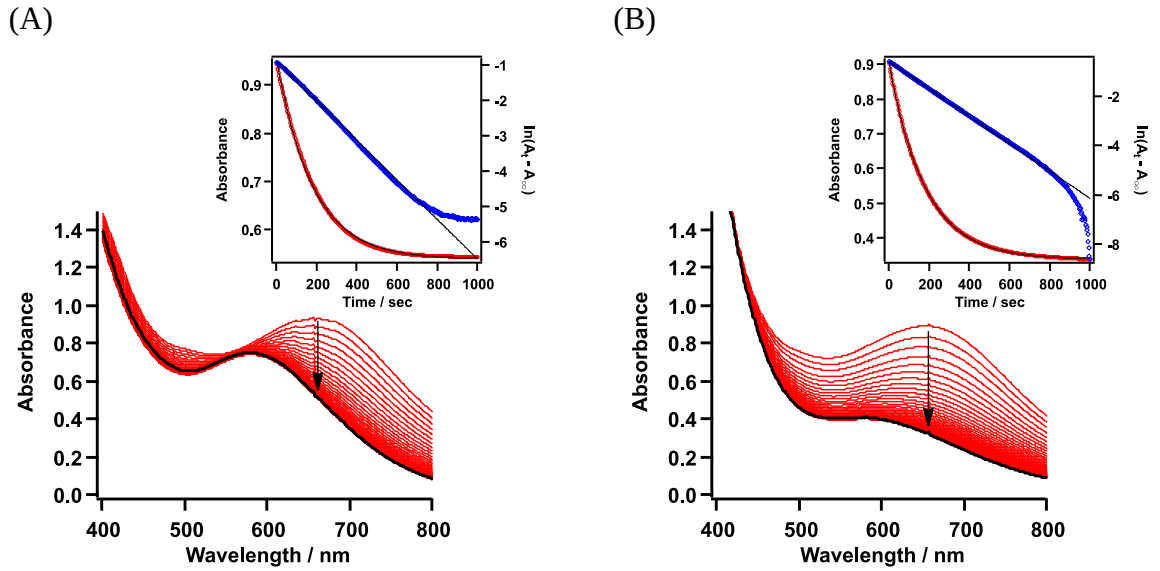

Figure S6. Electronic spectral change for decomposition of **1**-O_2 (0.56 mM) in the absence of benzyl alcohol (A) and in the presence of benzyl alcohol (0.56 M, 1000 equiv.) (B) in dichloromethane at 25 °C . Insets: Decay time profile of the absorbance at 668 nm (curve) and pseudo-first order plot (liner plot).

Table S2. Kinetic parameters for the reaction of **1**-O_2 with benzyl alcohol at 25 ºC.

[benzyl alcohol] / M	[**1**-O_2] / mM	[benzyl alcohol]/[**1**-O_2] / eq.	k_{obs} / s^{-1}
0	0.56	0	5.58×10^{-3}
0.06	0.55	100	5.73×10^{-3}
0.14	0.55	250	6.27×10^{-3}
0.27	0.53	500	5.63×10^{-3}
0.42	0.53	800	6.16×10^{-3}
0.56	0.56	1000	5.56×10^{-3}

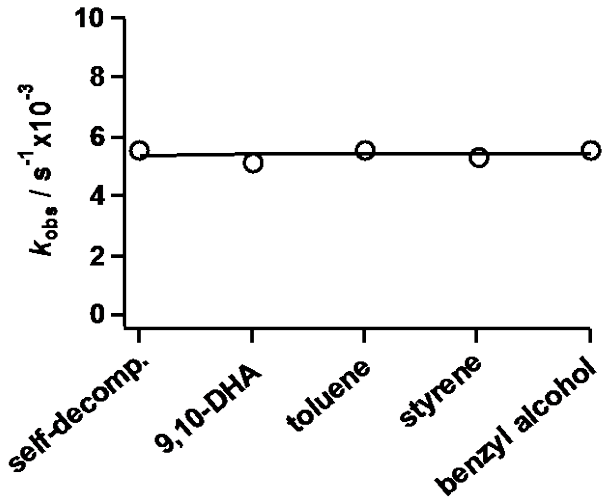

Figure S7. Plot of k_{obs} against concentrations of 9,10-DHA (0.17 M), toluene (0.52 M), styrene (0.52 M), and benzyl alcohol (0.56 M) in CH_2Cl_2 at 25˚C.

Table S3. Kinetic parameters for the reaction of **1**-O_2 with various substrates at 25 ºC.

substrates / M	[**1**-O_2] / mM	[substrate]/[**1**-O_2] / eq.	k_{obs} / s^{-1}
–	0.56	–	5.58×10^{-3}
9,10-DHA (0.17 M)	0.55	300	5.16×10^{-3}
toluene (0.52 M)	0.52	1000	5.57×10^{-3}
styrene (0.52 M)	0.52	1000	5.34×10^{-3}
benzyl alcohol (0.56M)	0.56	1000	5.56×10^{-3}

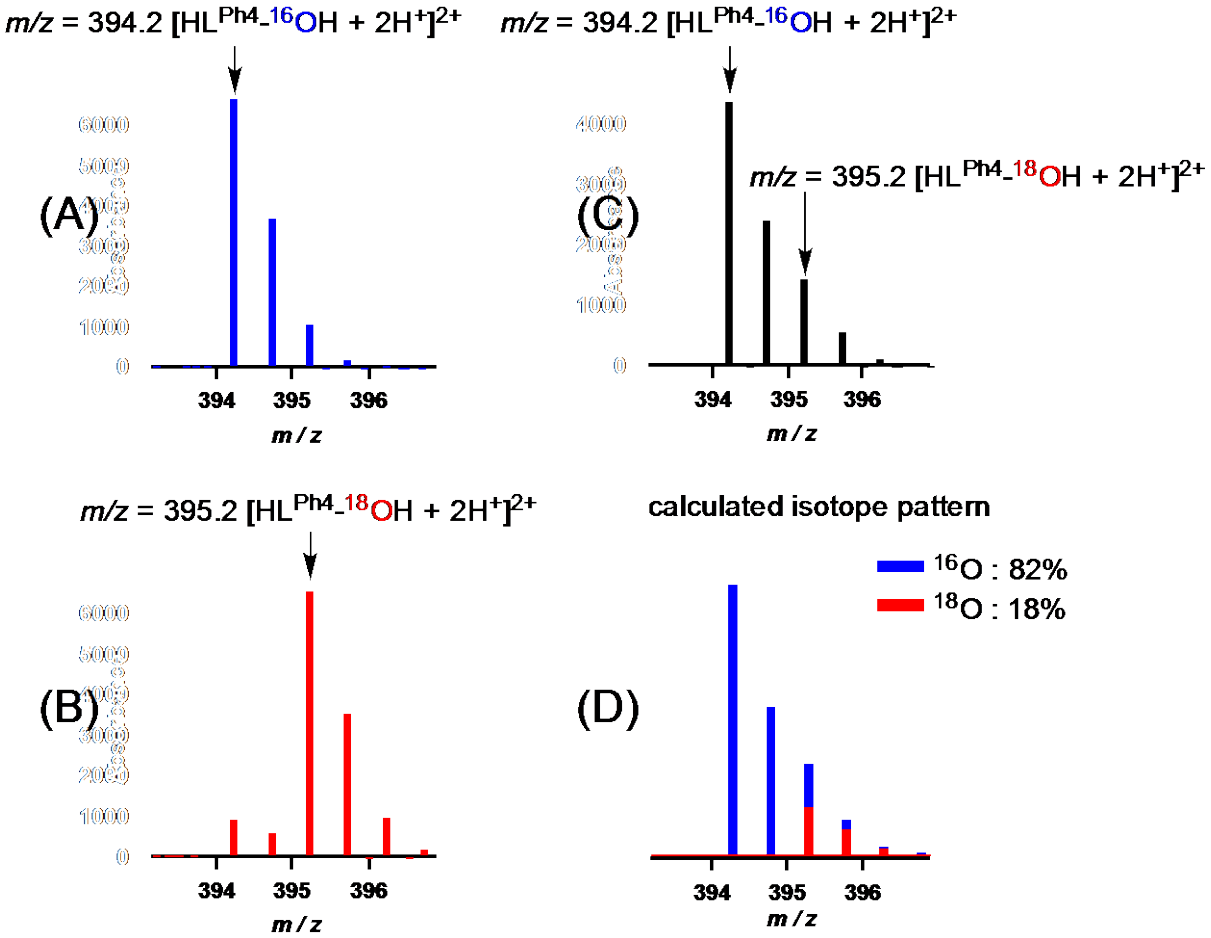

Figure S8. ESI-TOF mass spectra of HL^{Ph4}-^{16}OH (A), HL^{Ph4}-^{18}OH (B), and HL^{Ph4}-$^{16/18}OH$ (C) obtained from decomposed dichloromethane solutions of **1**-O_2 prepared by $^{16}O_2$, $^{18}O_2$, and $^{16}O_2$ in the presence of 1000 equiv. of $H_2{}^{18}O$ (diluted with MeCN) at 25 °C. (D) Calculated isotope pattern of (C).